Compressive Column Load Identification in Steel Space Frames Using Second-Order Deflection-Based Methods

Marco Bonopera[a,c*], Kuo-Chun Chang[b], Chun-Chung Chen[c], Tzu-Kang Lin[d], Nerio Tullini[a]

[a]*Department of Engineering, University of Ferrara, Ferrara, Italy*

[b]*Department of Civil Engineering, National Taiwan University, Taipei, Taiwan*

[c]*Bridge Division, National Center for Research on Earthquake Engineering, Taipei, Taiwan*

[d]*Department of Civil Engineering, National Chiao Tung University, Hsinchu City, Taiwan*

*Corresponding author - *E-mails:* marco.bonopera@unife.it - bonopera@ncree.narl.org.tw

Authors - *E-mails:* ciekuo@ntu.edu.tw - ccchen@ncree.narl.org.tw - tklin@nctu.edu.tw - nerio.tullini@unife.it

Abstract: This paper presents a comparison of two static nondestructive methods used to assess compressive loads in columns of steel space frames. The first method requires knowledge of the flexural rigidity of the column under investigation, whereas the second method requires knowledge of the column's buckling load. In each method, short-term displacements are measured at given cross sections along the member under examination, which is subjected to an additional transverse load. The two methods were verified in this study through experimental and numerical tests on a column of a small-scale space frame prototype with generic connections and end conditions. Estimations of compressive forces were generally reliable when second-order effects were accurately considered. In conclusion, the two methods can be successfully used to test steel space frames in a laboratory or under real conditions.

Keywords: inverse problem; nondestructive test; load identification; space frame.

1. Introduction

The identification of compressive column loads is required in steel space frames to support restoration projects or to ascertain how close a frame is to failure. Despite uncertainties regarding dead loads, an accurate evaluation of *in situ* compressive column forces is necessary for the safety

assessment of the entire space frame. Specifically, considerable internal force redistribution may indicate structural damage. Compressive load evaluation is also crucial for the safety assessment of steel storage pallet racks. In recent decades, advanced approaches for racks have been developed for estimating the key parameters governing static and seismic design.[1–6]

Axial load identification in slender beam-columns has been studied using static and dynamic nondestructive methods.[7–12] In particular, vibration-based estimations of axial loads in generic space frames require accurate selection of the flexural mode shape to be utilized in the identification process.[10,11] Such methods are particularly sensitive to experimental and model errors and it is also difficult selecting *a priori* the optimal frequency for estimating the compressive load. Moreover, different natural frequencies yield different degrees of accuracy in axial force estimations. A static approach to axial load identification in bar elements of simple prestressed trusses was investigated by Turco.[13] However, this nondestructive procedure considers only the axial stiffness of elements; thus, it cannot be applied to the columns of civil space frames or storage pallet racks, where rigid or semirigid joints must also be considered. Duan et al.[14] proposed the use of an elasto-magneto-electric sensor to directly and accurately identify axial force in steel cables. Specifically, this monitoring method is feasible only for new cable-stayed bridges, because the cables must be instrumented during construction. Similarly, structural health monitoring systems can be installed when completing the construction of a structure for continuous monitoring of structural responses.[15]

In this paper, the performance of two static nondestructive methods used for compressive load identification in generic space frames is compared. The first method extends the procedure proposed by Tullini[9] to steel space frames. Notably, this method was applied only on a steel tie-rod in a laboratory, and thus, no experimental verifications on beam-columns under compressive loads were obtained.[9] The corresponding algorithm can estimate the compressive force in a column by measuring five short-term displacements along the length of the column after applying a lateral load at the mid-span. Knowledge of the flexural rigidity of the column under examination is required, whereas the boundary conditions of the single member can be unknown. The second nondestructive

method in this study is based on the magnification factor method, which uses a simplified formula to estimate second-order displacements.[16,17] Specifically, the compressive axial load can be identified by measuring one short-term displacement along the column span when an additional lateral load is applied to the member. Knowledge of the Euler buckling load of the single column is the other fundamental requirement. The aforementioned methods use static parameters only; thus, in contrast to dynamic procedures, they do not require the selection of experimental data for use in the algorithms. Experimental and analytical tests conducted on a small-scale space frame prototype with generic connections and end conditions confirmed the robustness of both procedures. Therefore, both methods could be successfully applied in a laboratory or *in situ* on any slender column of a steel space frame or storage pallet rack, where in-plane bending with respect to a symmetrical axis must be exerted to avoid the coupling effects of bending and torsion.

2. Nondestructive Testing Methods

A prismatic column of a generic regular steel frame is considered (Fig. 1(a)). The reference model consists of a prismatic beam-column of length L constrained by two sets of end elastic springs whose parameters $k_{\varphi\varphi}^{(i)}$, $k_{v\varphi}^{(i)}$, and $k_{vv}^{(i)}$ (i = 0, 1) are collected by the 2 × 2 stiffness matrices $\mathbf{K}_0$ and $\mathbf{K}_1$ (Fig. 1(b)), because the extremities of a generic column can be subjected to displacements and rotations. The member is subjected to a compressive force N and an additional transverse load F located at a generic abscissa $x = a$ (Fig. 1(b)). The elastic modulus E and cross-sectional second moment of area I of each element of the frame are assumed to be known constants.

The formulations of the two nondestructive testing (NDT) methods presented in this study are described in the following sections.

2.1. NDT method 1: extension of the method proposed by Tullini[9]

In this section, the method proposed by Tullini[9] is extended to steel space frames. As mentioned, for the proposed method, no experimental verifications on beam-columns under compressive loads were obtained. The algorithm enables the estimation of the tensile or compressive load in a slender

beam-column by using five displacements measured along the column's length after a point load has been applied at the mid-span. Knowledge of the flexural rigidity *EI* of the prismatic beam-column is required, whereas the boundary conditions of the member of the space structure can be unknown. This aspect is crucial because the column extremities of a steel frame can generally be subjected to displacements and rotations and its length can be undefined because of the finite dimensions of the end joints (Fig. 1).

Following the application of the lateral load F at the mid-span (i.e., at $x = x_2$ in Fig. 1), five short-term displacements, v_0, v_1, v_2, v_3, and v_4, are recorded at the coordinates $x_0 = 0$, $x_1 = L/4$, $x_2 = L/2$, $x_3 = 3L/4$ and $x_4 = L$. The constant L is the length of the substructure along the column, where v_0 and v_4 are the deflections at the extremities of the assigned length L. With a positive sign being assigned to the compressive forces, the displacements v_0, v_1, v_2, v_3, and v_4 are used in the following transcendental equation to calculate the nondimensional compressive axial load $n = N L^2/EI$:

$$\frac{v_1 + v_3}{v_2} = \frac{\dfrac{v_0 + v_4}{2v_2} + 1 + 2\cos(\sqrt{n}/4)}{1 + \cos(\sqrt{n}/4)} + \frac{\psi}{4v_2} \frac{\sqrt{n}\cos(\sqrt{n}/4) - 4\sin(\sqrt{n}/4)}{\sqrt{n^3}\,[1 + \cos(\sqrt{n}/4)]} \tag{1}$$

where $\psi = FL^3/EI$ is the load parameter with a length dimension.

For simply supported members that are of length L and constrained by two end rotational springs, $v_0 = v_4 = 0$, and Eq. (1) is reduced to Eq. (10) reported in Tullini et al.[8]

In summary, load identification must conform to the following steps:

1) Evaluate the displacements v_0, v_1, v_2, v_3, and v_4 through a three-point bending test.

2) Solve transcendental Eq. (1) for the unknown constant n by using the ratios $(v_1 + v_3)/v_2$ and $(v_0 + v_4)/v_2$, as well as the expression for ψ.

3) Determine the analytical value $N_a = n\,EI/L^2$ of the compressive force.

2.2. NDT method 2: magnification factor method

During the execution of preliminary design computations for steel frames, access to an approximate formula for determining the displacements in columns under compressive axial loads is often useful. In particular, the total deflection v_{tot} is equal to the product of two terms[16,17]: the first-order deflection v_I (neglecting the effect of the compressive load) and a magnification factor $1/(1 - N/N_{crE})$, where N is the compressive force in the column and N_{crE} is the corresponding first Euler buckling load of the member, expressed as follows:

$$v_{tot} = \frac{v_I}{1 - N/N_{crE}}. \tag{2}$$

In general, the simplified formula can be used with high accuracy if the first-order deformed shape of the beam-column and the first buckling shape are similar.

Equation (2) can be used to estimate the compressive axial force in the column. After the load F is applied, one displacement $v_{tot} = v_i$ is recorded at the ith cross section, such as v_2 (Fig. 1). To identify the compressive load N, the simplified Eq. (2) can be rearranged as follows:

$$N = N_{crE}\left(1 - \frac{v_I}{v_{tot}}\right). \tag{3}$$

The first-order displacement v_I can be calculated analytically using a finite element (FE) model of the entire space frame or experimentally if it is possible to obtain the deflection v_I without second-order effects such as those during the construction of the civil frame or assembly of the storage pallet rack. Similarly, the Euler buckling load $N_{crE} = \pi^2 EI/l_0^2$ can be determined numerically using the adopted FE model or simplified formulas for braced or unbraced compression members, considering the restraints at the column ends and geometric and material properties of the frame, as expressed in Eqs. (5.15) and (5.16) of Eurocode 2.[18] In the experiments performed on a space frame prototype described in the next section, the effective length l_0 of the column under

examination was obtained using Eq. (5.16) of Eurocode 2[18] for isolated unbraced members with a constant cross section in regular frames, expressed as follows:

$$l_0 = L \cdot \max\left\{\sqrt{1+10\frac{k_0 \cdot k_4}{k_0+k_4}};\quad \left(1+\frac{k_0}{1+k_0}\right)\cdot\left(1+\frac{k_4}{1+k_4}\right)\right\}, \tag{4}$$

where k_0 and k_4 are the flexibilities of the rotational restraints at column ends 0 and 4, respectively.

Studies have proposed dynamic testing methods for determining the buckling load in frame structures.[19–26] Recently, Blostotsky et al.[27] improved the static test procedure proposed by Vaswani[28] for use in regular frames.

In summary, the process of the NDT method must conform to the following procedural steps:

1) Measure the displacement v_{tot} in a cross-section along the column span following the application of a point load F.

2) Use an FE model or simplified formulas to numerically determine the Euler buckling load N_{crE}.

3) Evaluate the first-order displacement v_{I} in the same cross section of the total displacement v_{tot} either experimentally, by conducting a preliminary test, or analytically, by applying an FE model, while considering the magnitude and position of the load F.

4) Determine the analytical compressive force N_a through Eq. (3).

Notably, the additional load F can be applied at different cross sections along the span, thereby underlining that the first-order displacement v_{I} and experimental displacement v_{tot} must be in reference to the same cross section.

3. Application of NDT Methods in a Space Frame Prototype

A space frame prototype with unknown connections was used to verify both NDT methods. The prototype had a height of L_C = 680 mm and beam spans of L_B = 400 mm, as shown in Fig. 2(a). The prototype was composed of slender beam-columns of aluminum alloy with a tube cross section of 10.0 mm in external diameter and 1.0 mm in tube thickness. The objective was to simulate the behavior of a steel space frame. The second moment of area for the tube cross section I_{exact} was

289.8 mm^4. All geometric dimensions of the frame prototype were verified by measuring systems of 0.01 mm tolerance (laser rangefinder and caliper) once the prototype had been fixed onto a steel table for laboratory testing (Fig. 2(b, c)). The yield stress, f_{yk} = 320 MPa, and elastic modulus, E = 74.13 GPa, of the aluminum alloy were experimentally evaluated. These parameters were identified as the mean values of tensile tests on three specimens with solid circular cross sections of 10 mm in diameter and 500 mm in length.

The space frame prototype had welded nodes (Fig. 2(b)). A rigid plastic plate was used to create support for the vertical load, which was necessary for experimental verifications (Fig. 2(b)). For both NDT methods, vertical loads were applied by adding cast iron bricks with known mass to the upper portion of the prototype (Fig. 2(b)), causing the resultant external load Q to split at the upper nodes and at the mid-span of the beams (Fig. 3). Two strain gauges were fixed at diametrically opposite positions close to the bases of the four columns (Fig. 2(c)). The corresponding strains were recorded every second for nearly 40 seconds by a data acquisition unit, in each experimental test combination. The mean value of the strain measures was used to evaluate the experimental compressive forces N_x. The transverse load F was applied by using an endless screw and measured with a 10 kN load cell of 2.0 mV/V accuracy. The space frame prototype was always preserved in the elastic range during the experimental and analytical verifications of both NDT methods.

3.1. Verifications of NDT method 1

In this section, the experimental and analytical tests of the method proposed by Tullini[9] are described. Four assigned compressive force N_x values were applied to the frame prototype through the external load Q, as presented in Table 1. For each assigned compressive force N_x, two equal and opposite forces F with initial values of 29.4 + 29.4 N were applied to the two columns at the mid-span; the initial values were then gradually increased to 58.8 + 58.8 and 68.6 + 68.6 N in order to investigate the compressive forces N_a of the right column (Fig. 3 and Table 1). This loading

condition can easily be made viable in a laboratory or *in situ* by stretching a cable between two steel columns and measuring the corresponding applied forces F.

3.1.1. Experimental testing

In the experimental verifications, the five short-term displacements v_0, v_1, v_2, v_3, and v_4 of the deflected shape of the right column were measured using dial indicators after each application of the transverse loads $F + F$ (Fig. 4(a, b, c)).

Two test configurations, both with substructure length $L = L_C = 680$ mm (Fig. 3), were considered. Test 1 entailed employing the three sensors located at cross sections 1, 2, and 3, assuming $v_0 = v_4 = 0$ and also assuming the existence of two rotational springs at the column ends only. By contrast, Test 2 entailed considering all five short-term total displacements and assuming the boundary conditions of the right column under investigation to be unknown. Table 1 presents the parameters measured for each combination used in Eq. (1) to identify the compressive loads N_a. The assumption of two end supports in the right column for Test 1 necessitated the proportional subtraction of displacement v_4 from displacements v_1, v_2, and v_3; specifically, v_1, v_2, and v_3 were replaced by $v_1 - v_4/4$, $v_2 - v_4/2$, and $v_3 - 3v_4/4$, respectively (Table 1). The maximum measured displacement, v_2, at the mid-span was less than $L_C/80$.

Table 2 shows the compressive column load evaluations N_a for Tests 1 and 2, with the evaluation errors being $\Delta = (N_a - N_x)/N_x$. A comparison of the estimated N_a and measured N_x values for both tests for each transverse load $F + F$ is presented in Figs. 5(a)–5(c). In general, Tests 1 and 2 yielded accurate approximations of the estimated compressive force N_a. These experiments provided load estimations of N_a with errors $\Delta < 10\%$ (in absolute value) when the right column of the prototype was subjected to compressive loads N_x with second-order effects of 45% of the total displacements and subjected to transverse loads $F > 58.8$ N; this is because the estimation accuracy increased when higher second-order effects were induced.

3.1.2. Analytical verification

An FE model of the space frame prototype was used to compute the five displacements v_0, v_1, v_2, v_3, and v_4 by conducting second-order static analysis without provision for any imperfections in the geometric model. The FE model adopted for the prototype uses four FEs for each beam and column, where Euler–Bernoulli beams adopting exact shape functions describing second-order effects are used.[17] Specifically, the frame prototype was loaded with point loads equal to $Q/8$ at the upper nodes and mid-span of the beams. Table 3 presents the displacements evaluated using the FE model and considering column flexural rigidity, $EI_{exact} = 74134 \times 289.8 = 2.148 \times 10^7$ Nmm^2, for five assigned compressive load N_x values and for $F = 68.6$ N.

To perform a sensitivity analysis, the displacements v_1, v_2, and v_3 in Test 1 and v_0, v_1, v_2, v_3, and v_4 in Test 2 were alternatively modified by adding +0.01 or −0.01 mm. The loads F were alternatively modified by adding +0.5 or −0.5 N in both tests to reproduce possible experimental errors. In total, 16 distinct combinations of simulated experimental values were obtained for Test 1 and 64 distinct combinations of simulated experimental values were obtained for Test 2. The combinations refer to the five distinct assumed compressive loads N_x for each test configuration. Figures 5(a)–5(c) depict a comparison of the worst estimated N_a and the assumed N_x values for Tests 1 and 2 in terms of sensitivity analyses when the loads were $F = 29.4$, 58.8, and 68.6 N. Test 1 yielded the most accurate approximation of the compressive axial load. When $F = 68.6$ N, the N_a values were between $N_x - 22$ N and $N_x + 18$ N. Test 2 also yielded accurate load estimates, because the N_a values were between $N_x - 19$ N and $N_x + 20$ N (Fig. 5(c)). Finally, the sensitivity analyses reported in Figs. 5(a)–5(c) confirm that generally, a good compressive load identification N_a can be obtained when the columns are subjected to larger lateral loads F, thereby increasing the transverse deflections due to the second-order effects.

3.2. Verifications of NDT method 2

The experimental verifications of the magnification factor method are presented in this section. For each vertical resultant load Q, a force F was applied at the top of the right column under

investigation (Fig. 6) and the short-term horizontal displacement v_{tot} at the same application point was recorded. Preliminary evaluations or FE spatial models are necessary to estimate the first-order displacement v_I and Euler buckling load N_{crE} of a single column.

3.2.1. Experimental testing

A first-order short-term displacement $v_{I,4}$ = 8.00 mm was recorded after the application of the horizontal load $F_{4,x2}$ = 14.7 N on the unloaded prototype. Notably, the second-order effects in the right column were negligible without a vertical load Q. The lateral force $F_{4,x2}$ did not engender significant second-order effects in terms of deflections (Figs. 7(a)–7(c)). Hence, the horizontal displacement $v_{I,4}$ can be considered a first-order displacement and can be used in Eq. (3) in the NDT method. Conversely, the short-term total displacements $v_{tot,4}$ were measured on the loaded prototype (Figs. 8(a) and 8(b)).

The buckling load of the right column was estimated using Euler's formula, $N_{crE,x2} = \pi^2 EI_{exact}/l_C^2$ = 386 N (Fig. 9(a)), where the effective length l_C = 1.09 L_C was obtained using Eq. (5.16) of Eurocode 2[18] for isolated unbraced members with constant cross section in regular frames, as reported in Eq. (4) in Section 2.2. The slenderness of the right column was equal to 231. The relative flexibilities k_0 and k_4 of the rotational restraints at column ends 0 and 4 are expressed as follows for the fixed and top node, respectively:

$$k_0 = 0, \qquad k_4 = \left(\frac{EI_{exact}}{L_C} \right) \cdot \left(\frac{L_B}{6EI_{exact}} \right). \tag{5}$$

The horizontal force $F_{4,x2}$ applied at the top of the column under investigation yielded a variation ΔN_x of the experimental compressive loads N_x due to the vertical load Q only. The resulting compressive forces $N_x - \Delta N_x$ were recorded by two strain gauges closely fixed to the base of the column axis, as produced in the experiments of the method proposed by Tullini.[9] Therefore, the percentage errors could be derived as follows: $\Delta = [N_a - (N_x - \Delta N_x)]/(N_x - \Delta N_x)$. Table 4 presents all measured and identified parameters of the method. Poor estimates of N_a were yielded

when nonsignificant second-order effects were induced, or more specifically, when $N_x - \Delta N_x < 99$ N. Conversely, in the final seven test combinations (Table 4), the load estimations yielded favorable results because the compressive loads N_a were identified with errors $\Delta < 10\%$ (in absolute value). In particular, the minimum compressive load $N_x - \Delta N_x = 99$ N, corresponding to the range of the reliable load identifications obtained (Table 4), was 25.6% of $N_{crE,x2} = 386$ N. Consequently, the first-order displacements were magnified by a factor greater than $1/(1 - (N_x - \Delta N_x)/N_{crE,x2}) = 1/(1 - 99/386) = 1/(1 - 0.256) = 1.34$ (Eq. (2)). Notably, for columns with singly symmetrical cross sections, such as structural elements in storage pallet racks, the applied loads must act along the symmetrical axis only.

3.2.2. Analytical verification of the buckling load

The FE model of the space frame prototype was used to calculate the vertical buckling load $Q_{crE,a2} = 1360$ N of the first mode shape, depicted in Fig. 9(b). The buckling load $N_{crE,a2} = 288$ N was subsequently obtained using the corresponding axial force in the right column under observation in the FE model by assigning the loading arrangement $Q_{crE,a2}$ and $F_{4,x2}$ and without providing any geometric imperfections. Specifically, the FE model uses four FEs for each member, where Euler–Bernoulli beams with exact shape functions that describe the second-order effects are adopted,[17] as in the previous verifications of the method proposed by Tullini.[9]

The adopted experimental value $N_{crE,x2} = 386$ N was 34% greater than the analytical $N_{crE,a2}$ value. The application of a non negligible transverse load $F_{4,x2}$ at one top node only reduced the buckling load $N_{crE,a2}$ of the right column. Nonetheless, an error of 34% in the estimate of N_{crE} with respect to the analytical buckling load of $N_{crE,a2} = 288$ N did not deteriorate the compressive load estimations N_a (Table 4), thereby confirming the robustness of the NDT method.

Figure 10(a) illustrates a plot of the experimental load Q versus displacement $v_{tot,4}$ until the buckling behavior of the prototype was attained. Similarly, Fig. 10(b) illustrates a plot of the

compressive right column load $N_x - \Delta N_x$ versus displacement $v_{tot,4}$. Finally, the parameters measured in the experiments were added to the plot.

4. Conclusions

Two NDT methods for the assessment of compressive column loads in steel space frames are described in this paper. Both procedures use short-term transverse displacements measured along the column under investigation after an additional lateral load has been applied with respect to a symmetrical axis. Load identifications are possible in the method proposed by Tullini,[9] even if the columns have uncertain lengths and boundary conditions; the accuracy of the load estimates increases when higher second-order effects are induced by larger transverse loads. Specifically, compressive loads that provide a magnification factor greater than 1.45 are required for gaining load estimation errors lower than 10%. Load identifications in the magnification factor method are based on a simplified formula,[16,17] and they also require significant second-order effects in the members. In this method, a load identification error lower than 10% can be obtained with a magnification factor greater than 1.34. Moreover, for columns with a singly symmetric cross section, providing a system for additional loading to bend the member only along its symmetrical axis is necessary. To preserve the elements in the elastic range, for both methods, a preliminary calculation of the required transverse load must be performed based on the geometrical and mechanical properties of the frame or storage pallet rack under investigation.

Acknowledgments

M.B. acknowledges the financial support of the "Tender for Young Researchers Abroad Grant" in 2014, provided by the University of Ferrara, Italy, and the "Summer Program in Taiwan Grant" in 2014 and 2015, provided by the Ministry of Science and Technology of Taiwan for European Ph.D. candidates. N.T. acknowledges the financial support of the "Research Program FAR 2017" provided by the University of Ferrara. The experiments were supported by funding from the National Applied Research Laboratories Project of Taiwan (NCREE-06104A1700). Finally, special gratitude is extended to the technicians and students of National Taiwan University, who provided considerable assistance to the authors.

References

1. Baldassino and C. Bernuzzi, Analysis and behaviour of steel storage pallet racks, *Thin Wall. Struct.*, **37** (2000) 277–304.
2. N. Baldassino and R. Zandonini, Design by testing of industrial racks, *Adv. Steel Constr.*, **7**(1) (2011) 27–47.
3. C. Bernuzzi, A. Gobetti, G. Gabbianelli and M. Simoncelli, Simplified approaches to design medium-rise unbraced steel storage pallet racks. I: elastic buckling analysis, *J. Struct. Eng.*, **141**(11) (2015).
4. C. Bernuzzi, A. Gobetti, G. Gabbianelli and M. Simoncelli, Simplified approaches to design medium-rise unbraced steel storage pallet racks. II: fundamental period estimates, *J. Struct. Eng.*, **141**(11) (2015).
5. C. Bernuzzi, A. Gobetti, G. Gabbianelli and M. Simoncelli, Unbraced pallet rack design in accordance with European practice–Part 1: selection of the method of analysis, *Thin Wall. Struct.*, **86** (2015) 185–207.
6. A. M. S. Freitas, M. S. R. Freitas and F. T. Souza, Analysis of steel storage rack columns, *J. Constr. Steel Res.*, **61** (2005) 1135–1146.
7. N. Tullini and F. Laudiero, Dynamic identification of beam axial loads using one flexural mode shape, *J. Sound Vib.*, **318**(1–2) (2008) 131–147.
8. N. Tullini, G. Rebecchi and F. Laudiero, Bending tests to estimate the axial force in tie-rods, *Mech. Res. Commun.*, **44** (2012) 57–64.
9. N. Tullini, Bending tests to estimate the axial force in slender beams with unknown boundary conditions, *Mech. Res. Commun.*, **53** (2013) 15–23.
10. A. S. Bahra and P. D. Greening, Identifying multiple axial load patterns using measured vibration data, *J. Sound Vib.*, **330**(15) (2011) 3591–3605.

11. K. Maes, J. Peeters, E. Reynders, G. Lombaert and G. De Roeck, Identification of axial forces in beam members by local vibration measurements, *J. Sound Vib.*, **332**(21) (2013) 5417–5432.

12. G. Rebecchi, N. Tullini and F. Laudiero, Estimate of the axial force in slender beams with unknown boundary conditions using one flexural mode shape, *J. Sound Vib.*, **332**(18) (2013) 4122–4135.

13. E. Turco, Identification of axial forces on statically indeterminate pin-jointed trusses by a nondestructive mechanical test, *Open Civil Eng. J.*, **7** (2013) 50–57.

14. Y. F. Duan, R. Zhang, C. Z. Dong, Y. Z. Luo, S. W. Or, Y. Zhao and K. Q. Fan, Development of Elasto-Magneto-Electric (EME) sensor for in-service cable force monitoring, *Int. J. Struct. Stab. Dy.*, **16** (2016) Article ID 1640016.

15. Y. Q. Ni and Y. X. Xia, Strain-based condition assessment of a suspension bridge instrumented with structural health monitoring system, *Int. J. Struct. Stab. Dy.*, **16** (2016) Article ID 1640027.

16. S. P. Timoshenko and J. M. Gere, *Theory of Elastic Stability* (McGraw-Hill, New York, 1961).

17. Z. P. Bazant and L. Cedolin, *Stability of Structures* (Oxford University Press, New York, 1991).

18. Eurocode 2, *Design of concrete structures - Part 1-1: General rules and rules for buildings* (2005).

19. W. E. Ayrton and J. Perry, *On struts. The Engineer* (Vol. 62, Dec.10: 464–465 and Dec. 24: 513–515, 1886).

20. R. V. Southwell, *On the analysis of experimental observations in problems of elastic stability* (Proc R Soc Ser A 135:601–616, 1932).

21. L. H. Donnell, *On the application of Southwell's method for the analysis of buckling tests* (In: Stephen Timoshenko 60th Anniversary Volume, the Macmillan Co., NY. 27–38, 1938).

22. M. J. Jacobson and M. L. Wenner, Predicting buckling loads from vibration data, *Exp. Mech.*, **8**(10) (1968) 35N–38N.
23. A. Segall and M. Baruch, A nondestructive dynamic method for the determination of the critical load of elastic columns, *Exp. Mech.*, **20** (1980) 285–288.
24. P. Lokkas, A search on the instability of frame structures tested to buckling under side sway, *Proceedings of the 4th GRACM Congress on Computational Mechanics GRACM 2002*, Patra, Greece, 27–29 June, Vol. 1, 284–290 (2002).
25. V. Kalaikumar, V. J. Kurian, S. P. Narayanan, M. S. Liew and A. B. Nabilah, Prediction of buckling load of steel racking frame using non-destructive method, *Proceedings of the 4th International Conference on Steel & Composite Structures* (2010).
26. B. Blostotsky and E. Efraim, Dynamic method for measuring critical buckling load of sway frames, *Proceedings of the 9th International Conference on Structural Dynamics – EURODYN 2014*, June 30 - July 2, Porto, Portugal, 3851–3856 (2014).
27. B. Blostotsky, E. Efraim and Y. Ribakov, Improving the reliability of measuring critical buckling load in sway mode frames, *Exp. Mech.*, **56** (2016) 311–321.
28. H. P. Vaswani, Model analysis method for determining buckling load of rectangular frames, *Exp. Mech.*, **1**(8) (1961) 55–64.

Table 1. Method proposed by Tullini.[9] Measured parameters for Tests 1 and 2.

			Test 1 (three-displacements)					Test 2 (five-displacements)				
$Q/4$ (N)	F (N)	N_x (N)	v_0 (mm)	v_1 (mm)	v_2 (mm)	v_3 (mm)	v_4 (mm)	v_0 (mm)	v_1 (mm)	v_2 (mm)	v_3 (mm)	v_4 (mm)
141	29.4	98	0	1.48	3.01	1.82	0	0	1.52	3.10	1.95	0.18
	58.8	119	0	3.85	5.80	2.45	0	0	3.88	5.86	2.54	0.12
	68.6	134	0	4.54	7.29	3.52	0	0	4.55	7.30	3.54	0.03
165	29.4	112	0	1.57	3.26	2.09	0	0	1.60	3.32	2.19	0.13
	58.8	141	0	3.11	6.49	4.15	0	0	3.17	6.60	4.32	0.23
	68.6	154	0	4.06	8.23	5.34	0	0	4.10	8.31	5.47	0.17
178	29.4	133	0	1.51	3.31	2.20	0	0	1.54	3.36	2.28	0.11
	58.8	168	0	3.12	6.69	4.42	0	0	3.16	6.78	4.55	0.18
	68.6	175	0	3.77	8.11	5.40	0	0	3.80	8.17	5.49	0.12
202	29.4	155	0	1.63	3.39	2.18	0	0	1.65	3.42	2.23	0.07
	58.8	186	0	3.24	6.98	4.65	0	0	3.26	7.02	4.71	0.08
	68.6	198	0	3.99	8.28	5.40	0	0	4.02	8.34	5.49	0.12

Table 2. Method proposed by Tullini.[9] Identified parameters and estimated N_a values for Tests 1 and 2.

			Test 1 (three-displacements)				Test 2 (five-displacements)					
$Q/4$ (N)	F (N)	N_x (N)	ψ (mm)	n	N_a (N)	Δ (%)	ψ/v_2	$(v_0+v_4)/v_2$	$(v_1+v_3)/v_2$	n	N_a (N)	Δ (%)
141	29.4	98	430	2.7	126	28.6	138.8	0.06	1.12	3.0	138	40.8
	58.8	119	861	2.3	109	-8.4	146.8	0.02	1.10	2.3	109	-8.4
	68.6	134	1004	3.1	144	7.5	137.5	0.00	1.11	3.0	140	4.5
165	29.4	112	430	3.0	137	22.3	129.6	0.04	1.14	2.8	128	14.3
	58.8	141	861	3.2	147	4.3	130.4	0.03	1.13	3.1	142	0.7
	68.6	154	1004	3.6	167	8.4	120.8	0.02	1.15	3.5	163	5.8
178	29.4	133	430	3.6	166	24.8	128.1	0.03	1.14	3.4	157	18.0
	58.8	168	861	3.3	156	-7.1	126.9	0.03	1.14	3.5	162	-3.6
	68.6	175	1004	4.2	193	10.3	122.9	0.01	1.14	4.2	193	10.3
202	29.4	155	430	4.0	186	20.0	125.8	0.02	1.13	3.8	178	14.8
	58.8	186	861	4.3	200	7.5	122.6	0.01	1.14	4.3	200	7.5
	68.6	198	1004	4.5	207	4.5	120.4	0.01	1.14	4.5	207	4.5

Table 3. Method proposed by Tullini.[9] Displacements computed by the FE model of the prototype using EI_{exact} for five assumed N_x values and transverse load of F = 68.6 N.

	$Q/4$ (N)	F (N)	N_x (N)	v_0 (mm)	v_1 (mm)	v_2 (mm)	v_3 (mm)	v_4 (mm)
FE model	40	68.6	40	0	3.41	7.31	4.88	0
FE model	80	68.6	80	0	3.51	7.54	5.03	0
FE model	120	68.6	120	0	3.62	7.77	5.20	0
FE model	160	68.6	160	0	3.73	8.03	5.38	0
FE model	200	68.6	200	0	3.85	8.29	5.58	0

Table 4. Magnification factor method. Estimated N_a values. All measured and identified parameters.

$N_{crE,x2}$ (N)	$F_{4,x2}$ (N)	$v_{I,4}$ (mm)	$Q/4$ (N)	$N_x - \Delta N_x$ (N)	$v_{tot,4}$ (mm)	N_a (N)	Δ (%)
386	14.7	8.00	32	56	9.10	47	-16.7
386	14.7	8.00	80	99	10.45	90	-8.6
386	14.7	8.00	92	108	11.43	116	7.3
386	14.7	8.00	104	115	12.04	130	12.6
386	14.7	8.00	116	127	12.50	139	9.4
386	14.7	8.00	128	137	12.81	145	5.8
386	14.7	8.00	140	155	13.11	150	-2.9
386	14.7	8.00	152	161	13.65	160	-0.8

List of Figures

Fig. 10. (a) Plot of vertical load Q versus displacement $v_{\mathrm{tot},4}$. (b) Plot of compressive right column load $N_x - \Delta N_x$ versus displacement $v_{\mathrm{tot},4}$. Symbols ○ represent parameters measured in the experimental tests.

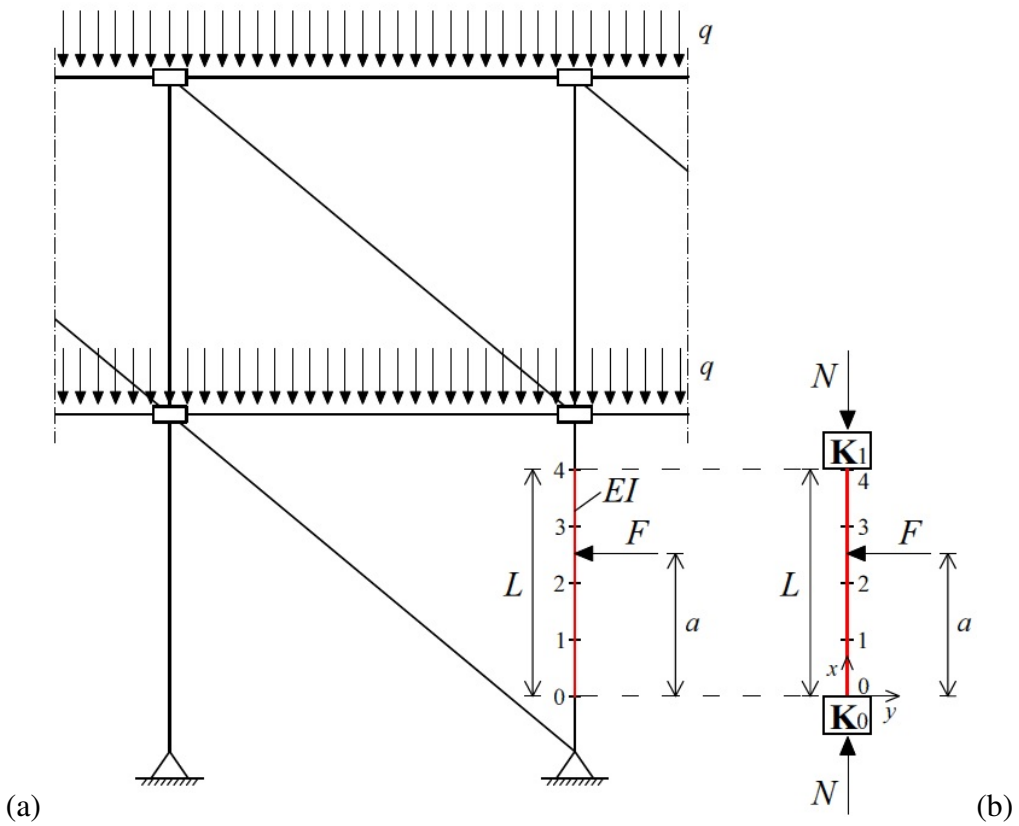

Fig. 1. (a) Prismatic column of a generic regular steel frame and (b) reference model with locations of instrumented sections.

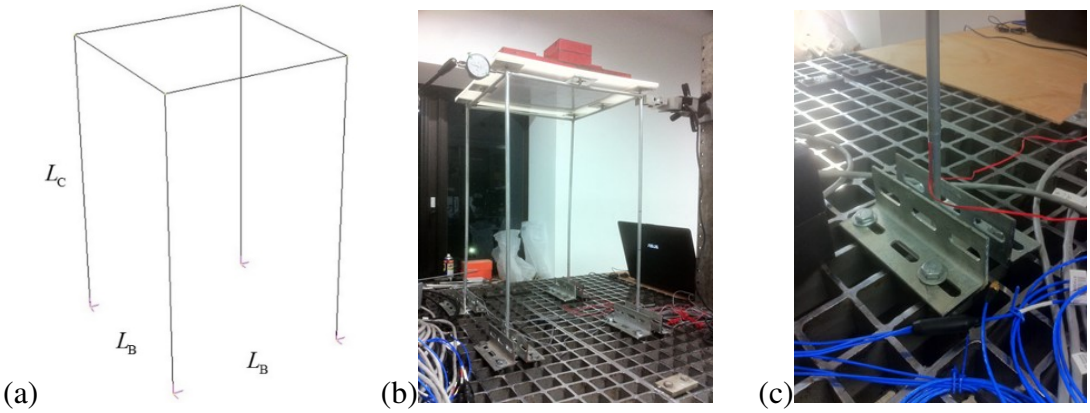

Fig. 2. Space frame prototype. (a) Scheme. (b) Steel table for experimental tests. (c) Fixed restraint and two strain gauges positioned close to the base of the column.

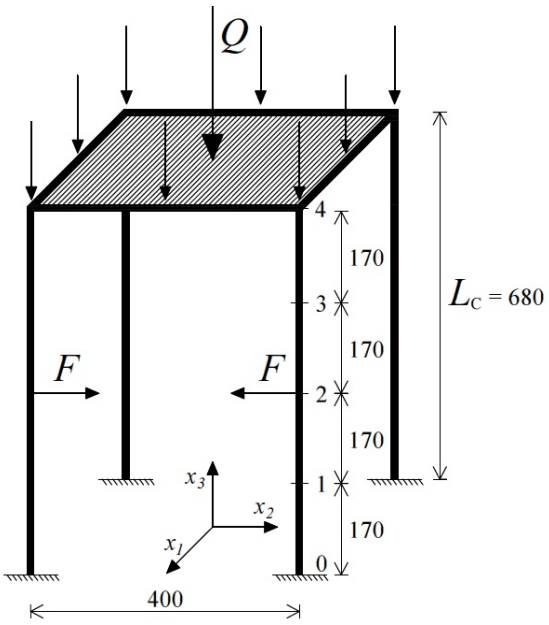

Fig. 3. Method proposed by Tullini.[9] Layout verification tests with locations of instrumented sections. Units: mm.

(a)  (b)  (c) 

Fig. 4. Method proposed by Tullini.[9] (a) Bending tests with three and five measurements performed concurrently. (b) Vertical load with symmetrical layout. (c) Deflection of right column and arrangement of dial indicators.

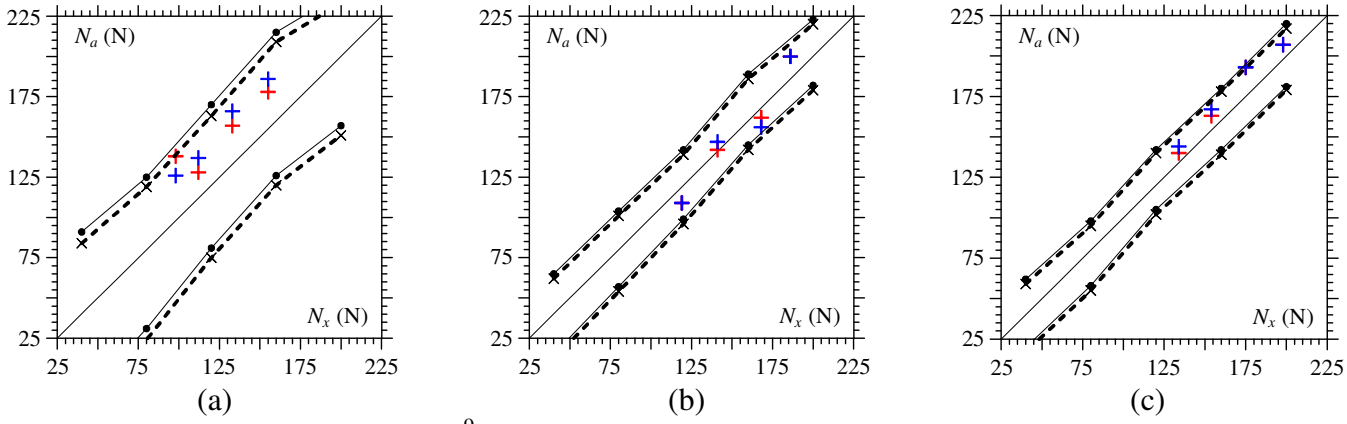

Fig. 5. Method proposed by Tullini.[9] Comparison of estimated N_a and measured N_x values for Test 1 (blue points) and Test 2 (red points) when F = (a) 29.4 N, (b) 58.8 N, and (c) 68.6 N. Dashed lines with symbol × and solid lines with symbol • refer to the sensitivity analyses for Tests 1 and 2, respectively.

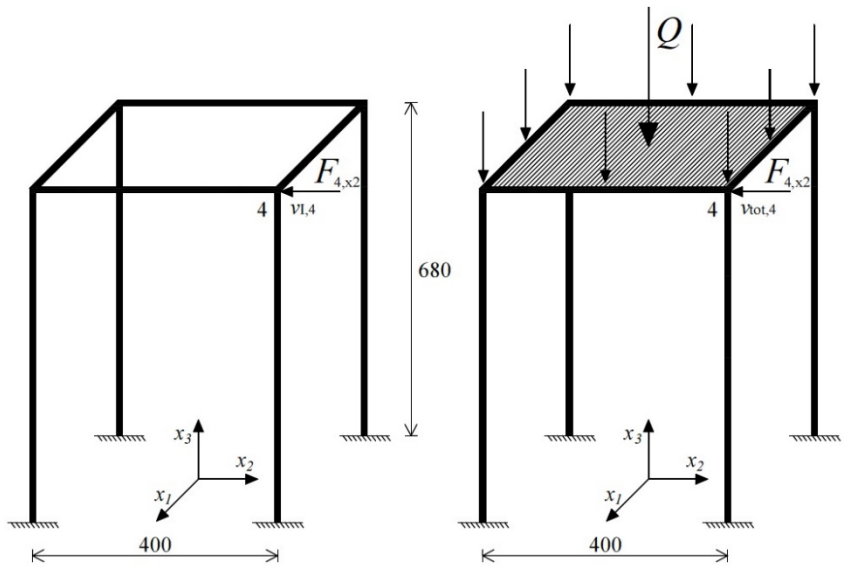

Fig. 6. Magnification factor method. Unloaded (left) and loaded (right) space frame prototypes. Layout verification tests, with the instrumented section being located at point 4. Units: mm.

(a)  (b) 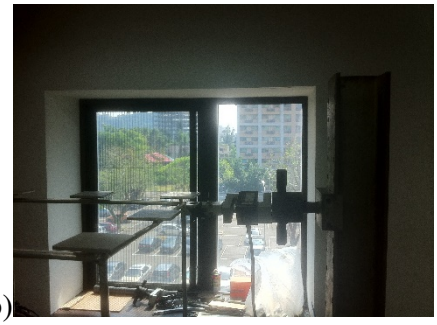 (c) 

Fig. 7. Magnification factor method and unloaded space frame prototype. (a) View of experimental testing. (b) Lateral load $F_{4,x2}$ applied by the endless screw and measured using a load cell. (c) Arrangement of dial indicator at the top node.

(a)  (b) 

Fig. 8. Magnification factor method and loaded space frame prototype. (a) View of experimental testing. (b) Lateral load $F_{4,x2}$ applied by an endless screw and measured using a load cell.

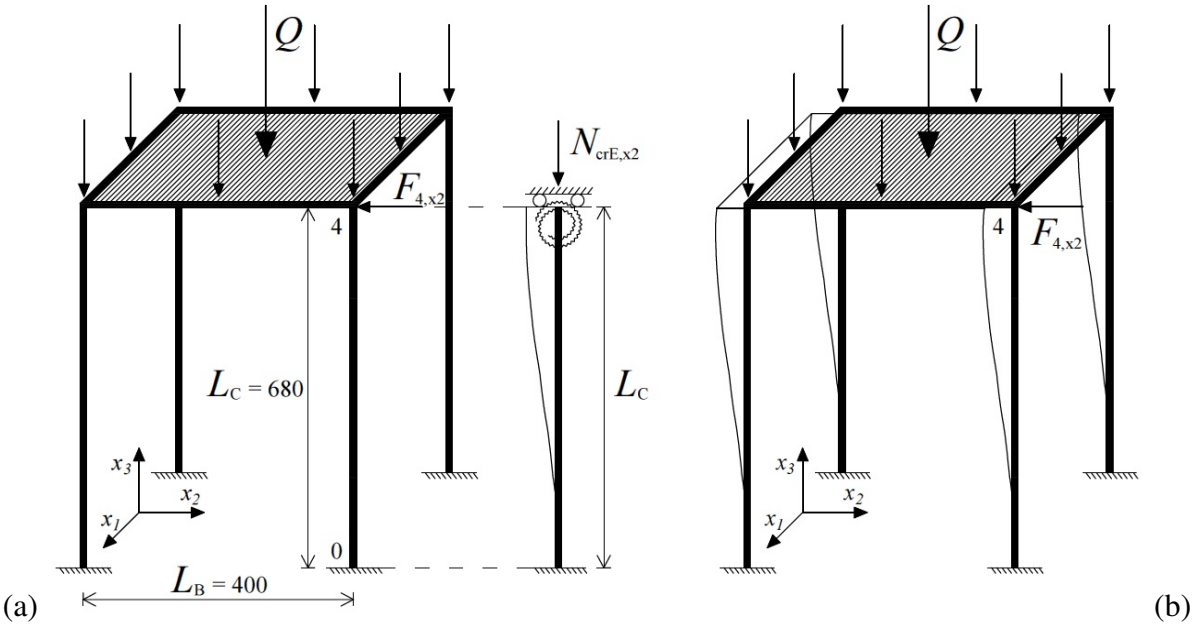

Fig. 9. Magnification factor method. (a) Reference model of the right column assumed to be an isolated unbraced member. (b) First numerical buckling shape of the space frame prototype.

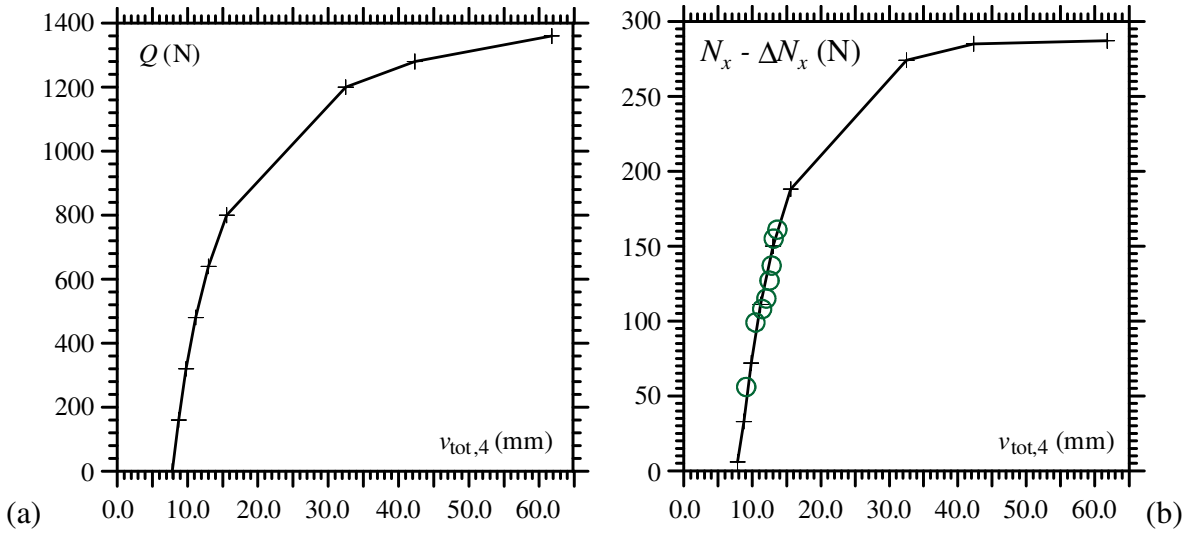

Fig. 10. (a) Plot of vertical load Q versus displacement $v_{tot,4}$. (b) Plot of compressive right column load $N_x - \Delta N_x$ versus displacement $v_{tot,4}$. Symbols ○ represent parameters measured in the experimental tests.